EDGE ARTICLE

Check for updates

Metal-catalyzed B–H acylmethylation of pyridylcarboranes: access to carborane-fused indoliziniums and quinoliziniums†

Hou-Ji Cao, Xing Wei, Fangxiang Sun, Xiaolei Zhang,* Changsheng Lu [ID] * and Hong Yan [ID] *

Metal-catalyzed mono-acylmethylation of pyridylcarboranes has been realized using α-carbonyl sulfoxonium ylides as a coupling partner. The reaction features high efficiency, excellent site-selectivity and good functional group tolerance. In the presence of pyridyl and enolizable acylmethyl groups, a post-coordination mode has been proposed and validated by *in situ* high resolution mass spectroscopy (HRMS) to rationalize the unique mono-substitution. Post-functionalization at the newly incorporated alkyl site provides additional utility of this method, including the construction of carborane-fused indoliziniums and quinoliziniums. We believe that these mono-alkylated carboranes, together with their post-functionalized derivatives, may find applications in luminescent materials and drug discovery in the near future.

Introduction

Icosahedral carboranes are molecular clusters[1] that have triggered abundant research interest for decades as building blocks to construct versatile ligands,[2] functional materials[3] and tunable pharmacophores.[4] The development of new methodologies to incorporate organic functionalities into carboranes holds great promise at the interface between cluster chemistry and organic chemistry. Central to the derivatization of carboranes has been metal-catalyzed B–H functionalization to generate B–C bonds.[5] This strategy has emerged as a powerful strategy to provide otherwise inaccessible cluster molecules featuring mild reaction conditions, good functional group tolerance and improved step economy. Widely reported reactions include arylation, alkenylation, and alkynylation, while alkylation reactions that enable the formation of B–C(sp³) bonds have been less developed (Scheme 1a).[5,6] Pioneering examples of the development of cage boron alkylated carboranes include electrophilic total-methylation of *o*-carborane, *p*-carborane or the mono-carborane anion $[CB_{11}H_{12}]^-$ with methyl triflate[6a,b] and transition metal-mediated hydroboration of alkenes with carboranes,[6c] followed by recent reports of
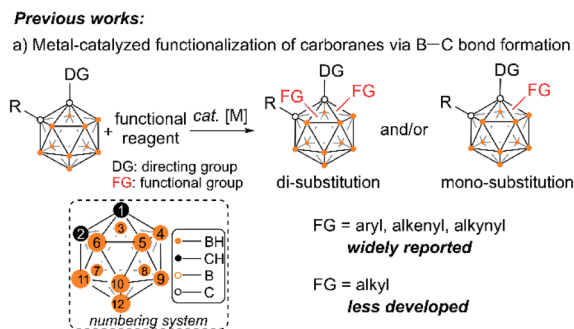
transition-metal catalysis[6d] and nucleophilic substitutions.[6e,f] A fundamental issue in this direction is how to control the mono-substitution when two or more chemically similar B–H bonds exist in the carborane cluster. Even now, it is still challenging to suppress the double functionalization and drive the reaction in a mono-functionalized direction, presumably owing to uncontrolled metal reactivity including the "cage walking" behavior.[7] Generally, stoichiometric control has been utilized to obtain one-fold functionalized products, although more-than-one-fold functionalized products can be usually generated.[5] In particular, carboranes with mono-alkylated substituents[4d–f,8] are highly desirable considering their utility for precise post-functionalization (such as cross-coupling reaction, annulation, bio-conjugation, *etc.*) at the alkyl site. In this work, readily accessible α-carbonyl sulfoxonium ylides[9] have been utilized for the development of a general Rh(III)Cp*-catalyzed selective alkylation of cage B–H bonds of 1-(2-pyridyl)-carboranes. It is noteworthy that metal–carbene intermediates in which sulfoxonium ylides function as precursors are known to undergo X–H (X = N, O, S, C) bond insertion reactions,[9] while insertion into the B–H bonds of carboranes is yet to be established. A post-coordinating mode has been proposed to control the mono-substitution in metal-catalyzed B–H activation.

With this strategy, a vast number of mono-acylmethylated carboranes have been synthesized in high yields with excellent B(4)-vertex selectivity with the aid of the pyridyl directing group (Scheme 1b). The synthetic utility of these mono-acylmethylated pyridylcarboranes allows for the construction of carborane-fused heteroarenes including indoliziniums and quinoliziniums with carboranyl fusion. It is known that cationic heteroarenes are well-established DNA binders that can affect

State Key Laboratory of Coordination Chemistry, Jiangsu Key Laboratory of Advanced Organic Materials, School of Chemistry and Chemical Engineering, Nanjing University, Nanjing, Jiangsu 210023, P. R. China. E-mail: hyan1965@nju.edu.cn; zhangxiaolei1213@yahoo.com; luchsh@nju.edu.cn

Previous works:

a) Metal-catalyzed functionalization of carboranes via B–C bond formation

Scheme 1 Metal-catalyzed B–H functionalization of carboranes via B–C bond formation.

synthetic utility of these mono-alkylated products, we have realized the intramolecular annulation between the remaining pyridyl and newly attached alkyl groups to produce indoliziniums or quinoliziniums containing a five- or six-membered heterocycle. These carborane-fused indoliziniums or quinoliziniums represent a new type of boron-containing heteroarene.

Results and discussion

The reaction development is summarized in Table 1. At the outset of our studies, we chose 1-(2-pyridyl)-2-Me-o-carborane[2l] **1a** and α-carbonyl sulfoxonium ylide **2a** as the model substrates. In the presence of 6 mol% of [RhCp*Cl$_2$]$_2$, the treatment of **1a** with 2 equiv. of **2a** in the absence of any additives in HFIP at 100 °C for 18 h afforded the B(4)/B(5)-mono-acylmethylated product **3a** in an isolated yield of 72% (entry 1), and no di-acylmethylated product was observed. Attempts to replace the rhodium catalyst with either CoCp*(CO)I$_2$, [IrCp*Cl$_2$]$_2$ or Cu(CH$_3$CN)$_4$PF$_6$ were unsuccessful, while RhCp*(OAc)$_2$·H$_2$O and [Ru(p-cymene)Cl$_2$]$_2$ led to lower yields (entries 2–4). Introduction of Lewis bases or acids such as NaOAc or PivOH as an additive proved to be detrimental (entries 5 and 6). A prolonged or shortened period has little effect on yield (entries 7 and 8). At lower or higher temperature, the results were found to be slightly inferior to those observed under the standard conditions (entries 9 and 10). When other solvents such as toluene, 1,4-dioxane, DCE, THF, and CH$_3$CN were used, no desired

the biological activities of DNA.[10] In particular, cationic quinolizinium alkaloids berberine and its derivatives (Scheme 2) exhibit antimalarial properties and other biological activities.[11] Furthermore, drug design based on annulated indolizinium and quinolizinium derivatives (e.g. rhodacyanine derivatives) has attracted considerable attention.[12] In extending the
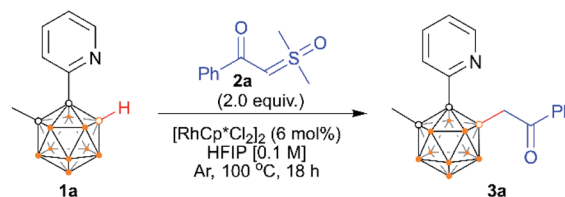
Table 1 Reaction development[a]

Entry	Variation from the standard conditions	Yield[b] [%]
1	None	77 (72)[c]
2	CoCp*(CO)I$_2$, [IrCp*Cl$_2$]$_2$, Cu(CH$_3$CN)$_4$PF$_6$ instead of [RhCp*Cl$_2$]$_2$	0
3	RhCp*(OAc)$_2$·H$_2$O instead of [RhCp*Cl$_2$]$_2$	59
4	[Ru(p-cymene)Cl$_2$]$_2$ instead of [RhCp*Cl$_2$]$_2$	63
5	With 1.0 equiv. of NaOAC	58
6	With 1.0 equiv. of PivOH	40
7	36 h instead of 18 h	76
8	12 h instead of 18 h	74
9	120 °C instead of 100 °C	74
10	80 °C instead of 100 °C	65
11	1.5 equiv. of **2a**, 36 h	73
12	3 mol% [RhCp*Cl$_2$]$_2$	60
13	Without [RhCp*Cl$_2$]$_2$	0
14	Under air	63

[a] Reaction conditions: **1a** (0.1 mmol), **2a** (0.2 mmol), [RhCp*Cl$_2$]$_2$ (6 mol%), HFIP (1.0 mL), 100 °C, Ar, 18 h. [b] Determined by ^{1}H NMR analysis of the crude reaction mixture. [c] Isolated yield. HFIP: hexafluoroisopropanol.

Scheme 2 Illustration of indoliziniums, quinoliziniums and carborane-fuse analogues.

product was detected, even though TFE led to trace **3a** (Table S1†). Reduction of **2a** to 1.5 equiv. led to **3a** in a slightly lower yield, even with a prolonged time period (entry 11). On the other hand, a lower yield was obtained when the catalyst loading was reduced (entry 12). Removal of the catalyst completely stopped the reaction (entry 13). It is noteworthy that the reaction still afforded a good yield when set up in an air atmosphere, which indicates that the method is rather robust (entry 14). In view of the yield, entry 1 was chosen as the optimal reaction conditions.

We then evaluated the scope of (hetero)aryl-substituted sulfoxonium ylides **2a–2z** with **1a** as a model substrate (Scheme 3). Substrates bearing electronically diverse substituents at different positions of the phenyl group were compatible, giving the corresponding products in moderate to excellent yields. Aryl sulfoxonium ylides having electron-donating groups such as –Me, –OMe, –OCF$_3$ and –CONHPh provided products (**3b–3d** and **3r**) in excellent yields (79–91%), despite the presence of reactive hydrogen. The lower yield for the substrate bearing
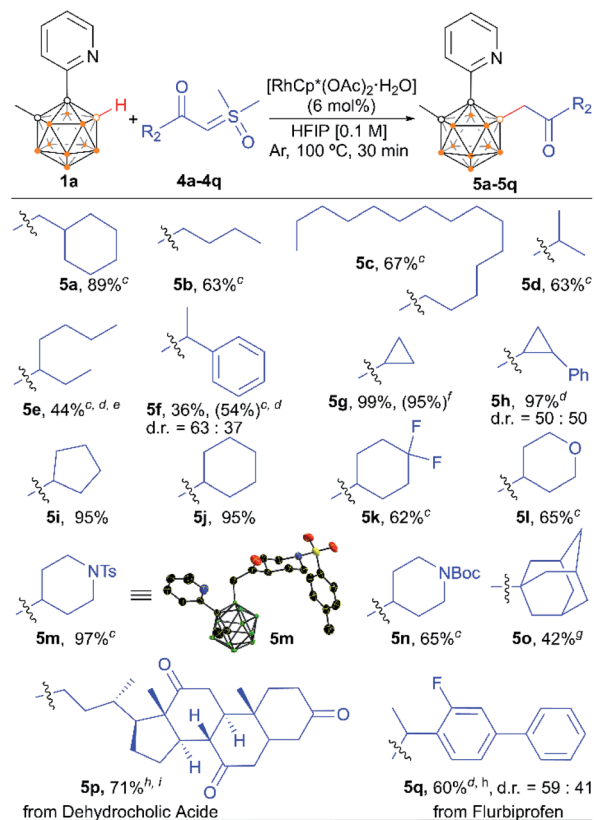
–SCF$_3$ may be attributed to its toxicity to the catalyst (**3e**). Notably, valuable halogen functional groups and ethers were well tolerated to afford the corresponding products in moderate to good yields which enables the late-stage manipulation of the initial products (**3c, 3d, 3f–3i, 3n, 3p** and **3s**). Furthermore, aryl sulfoxonium ylides bearing electron-withdrawing –CF$_3$, –Ph and –CO$_2$Me furnished **3j–3l** in moderate to good yields. Ylides having substituents at the *ortho-* or *meta*-position were all well tolerated (**3m–3p**). Substrates bearing multiple substituents were also examined, and the yields were comparable to those of the monosubstituted substrates (**3q** and **3s**). Naphthalen-1-yl- and naphthalen-2-yl-substituted sulfoxonium ylides were applicable to the present method, affording 78% and 70% yields, respectively (**3t** and **3u**). Substrates bearing furan scaffolds were effectively transformed into their corresponding products **3v** (>97%) and **3x** (60%). Similarly, thiophene and benzothiophene were compatible with the cross-coupling reaction (**3w** and **3y**). Furthermore, reaction of **1a** with adapalene[13] derived sulfoxonium ylide afforded the adapalene analogue **3z**, suggesting the potential of late-stage incorporation of the carboranyl motif into drug molecules using this reaction.

The scope of the alkyl-substituted sulfoxonium ylide coupling partners was also investigated (Scheme 4). With **1a** as the model substrate, the coupling reactions with aliphatic

Scheme 3 Scope of (hetero)aryl-substituted sulfoxonium ylides. [a] Reaction conditions: **1a** (0.1 mmol), **2a–2z** (2.0 equiv.), [RhCp*Cl$_2$]$_2$ (6 mol%), HFIP (1.0 mL), 100 °C, 18 h, Ar atmosphere. [b] Isolated yield. [c] [Ru(*p*-cymene)Cl$_2$]$_2$ (6 mol%) as a catalyst. [d] With achiral coupling partners, the products are obtained as a racemic mixture because reaction at the B(4) and B(5) positions occurs with equal probability, and no attempts were made to separate any of the B(4)/B(5) isomers of the entire product series.

Scheme 4 Scope of alkyl-substituted sulfoxonium ylides. [a] Reaction conditions: **1a** (0.1 mmol), **4a–4q** (2.0 equiv.), RhCp*(OAc)$_2$·H$_2$O (6 mol%), HFIP (1.0 mL), 100 °C, 30 min, Ar atmosphere. [b] Isolated yield. [c] 12 h. [d] Sulfoxonium ylide was used as a racemic mixture. [e] no d.r. was determined. [f] 1 mmol scale. [g] 48 h. [h] 3 h. [i] Enantiopure **4p** was used.

sulfoxonium ylides smoothly led to the desired products in moderate to excellent yields. Both primary and secondary aliphatic acid derived ylides exhibited good to excellent reactivity (**5a–5n**). In addition, the sterically hindered tertiary alkyl-substituted sulfoxonium ylide could also give the desired product (**5o**). Piperidine units, key structural motifs in numerous natural products and pharmaceuticals, were well tolerated (**5m** and **5n**). Tetrahydropyran was also a supportive motif (**5l**). Interestingly, cyclic secondary alkyl group containing substrates were converted into the respective products in nearly quantitative yields within 30 min (**5g–5j**). To showcase the practicality of the strategy, a scale-up reaction of **1a** and **4g** at a 1 mmol scale gave **5g** with a comparable yield.

We also examined the scope of the reaction by varying the carbon substituents in 1-(2-pyridyl)-2-R_1-o-carboranes using **4g** as the model substrate (Scheme 5). Gratifyingly, the carborane substrates bearing different substituents at the cage C(2) position afforded the B(4)/B(5)-mono-substituted products (**6b–6f**) in nearly quantitative yields, indicating that the carbon substituent effect did not influence efficiency and selectivity in this reaction. In addition, substitution on the 2-pyridyl ring (–F, –Me and –OMe) did not affect the outcomes, giving **6g–6i** in excellent yields. However, replacing the 2-pyridyl group with a phenyl or 3-pyridyl group totally shut down the reaction, which sheds light on the directing function of the 2-pyridyl moiety on the metal catalyst to activate the B–H bonds (ESI
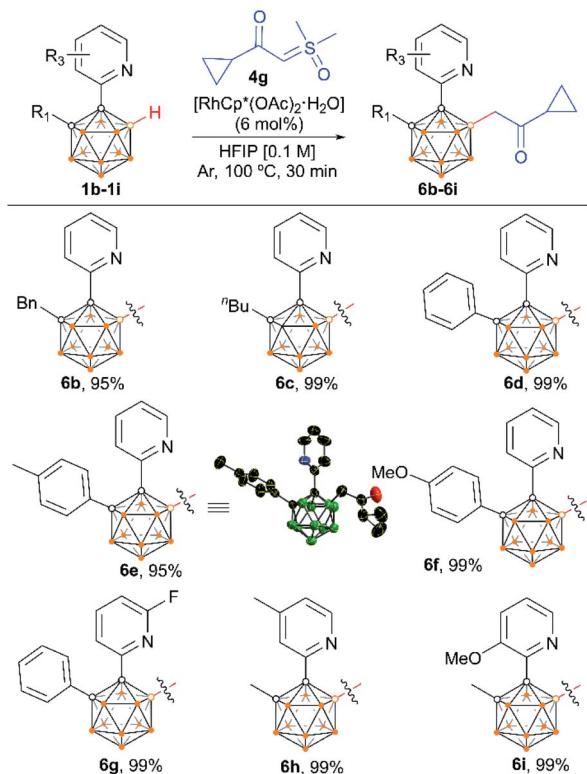
Scheme 5 Scope of o-carboranyl with various carbon-substituents.
[a] Reaction conditions: **1b–1i** (0.1 mmol), **4g** (2.0 equiv.), RhCp*(OAc)$_2$·H$_2$O (6 mol%), HFIP (1.0 mL), 100 °C, 30 min, Ar atmosphere. [b] Isolated yield.
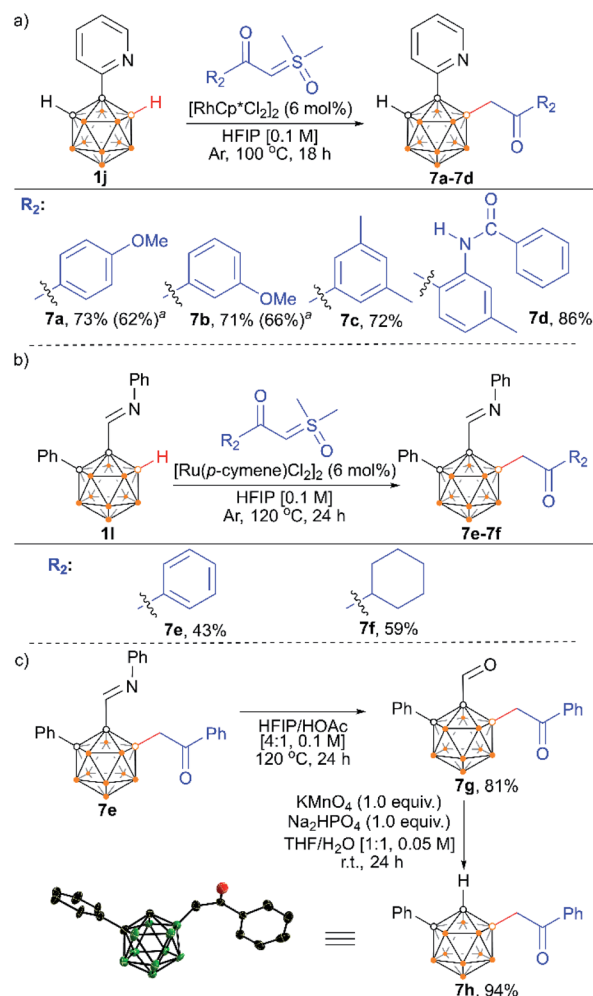
Scheme 6 Reactions of 1-(2-pyridyl)–o-carborane and o-carboranyl N-arylimine with α-carbonyl sulfoxonium ylides (a and b). Directing group removal (c). [a] [Ru(p-cymene)Cl$_2$]$_2$ (6 mol%) as a catalyst.

Schemes S8 and S9†). 1-(2-Pyridyl)-o-carborane and 1-(2-pyridyl)-p-carborane with free CH groups were also tolerated in this reaction, giving B(4)/B(5)-mono-acylmethylated products **7a–7d** and corresponding *para*-carboranyl derivatives as the major products (Schemes 6a and 7). In these reactions, the post-coordination effect also plays a significant role in controlling
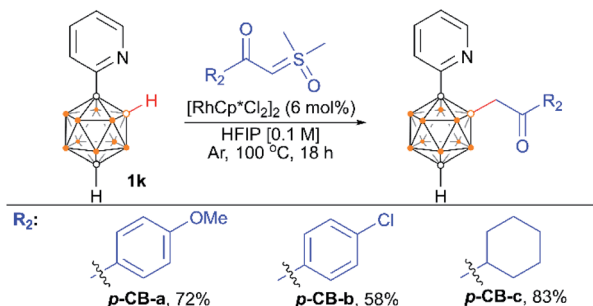
Scheme 7 Reactions of 1-(2-pyridyl)–p-carborane with α-carbonyl sulfoxonium ylides.

a)

1a
1a : 2c : 2l = 1 : 2 : 2

3c: R' = OMe, 90% (NMR yield)
3l: R' = CO$_2$Me, 10% (NMR yield)

b)

1a
1a : 2a : 4g = 1 : 2 : 2

5g: 97% (by NMR)
sole product

c)

1a
1a : 4g = 1 : 2

5g-D$_2$, 73%
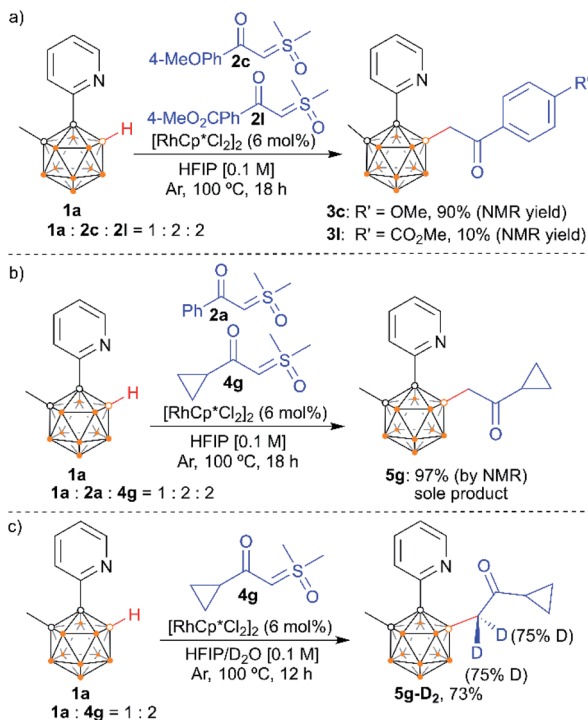
Scheme 8 Intermolecular competition experiments (a and b) and deuteration reaction (c).

the mono-substitution since the selectivity is usually low for the metal-catalyzed B–H functionalization reactions of *o*-carborane substrates with a free CH group.[5a,6a,6i] Interestingly, imine can also act as an effective directing group in the mono-acylmethylation reaction when using a ruthenium catalyst, giving corresponding products **7e** and **7f** in good yields (Scheme 6b). Furthermore, the imine group in **7e** can be readily removed after treatment with HOAc in HFIP, affording aldehyde **7g** in 81% yield (Scheme 6c). Subsequent removal of the aldehyde group in the presence of KMnO$_4$ (1.0 equiv.) and Na$_2$HPO$_4$ (1.0 equiv.) led to **7h** with a recovered CH site in 94% yield. In addition, competition experiments between ylides were examined as well. The B(4)–H alkylation between electron-rich (4-methoxy)- and electron-deficient (4-methoxycarbonyl) phenyl-sulfonium ylides (**2c** and **2l**) provided **3c** and **3l** in 90% and 10% yields, respectively, indicating that the electron donating effect on the phenyl group of phenylsulfoxonium ylide is dominant (Scheme 8a). Competition experiments between phenylsulfoxonium ylide (**2a**) and cyclopropylsulfoxonium ylide (**4g**) gave **5g** as the sole product in quantitative yield, demonstrating that alkylated sulfoxonium ylides **4g** is more reactive than **2a** (Scheme 8b).

To gain insights into the reaction mechanism, control experiments were performed. The reactions in the presence of a radical quencher, TEMPO or 1,1-diphenylethylene, still provided product **5g** in high yields (ESI Scheme S7†), implying that radical intermediates are not involved. The reaction of **1a** and **4g** under standard conditions (100 °C) in a mixed solution of D$_2$O and HFIP led to the incorporation of deuterium at the α-carbon with a deuterium level of 75% (Scheme 8c). This result is

in line with an *in situ* monitoring of the reaction in deuterated solvent HFIP-D$_2$ at 25 °C, which led to increased deuterium incorporation (>95%), albeit with slightly decreased conversion (ESI Fig. S30†). These results indicate a facile enolization process at the newly incorporated acylmethyl group attached to boron.[14] In sharp contrast, stirring **5g** in D$_2$O and HFIP at 25 °C in the absence of any other reagent or catalyst is not sufficient to enable deuterium incorporation at the enolizable positions. All of this demonstrates a reversible enolization and coordination process of the product with the rhodium catalyst.
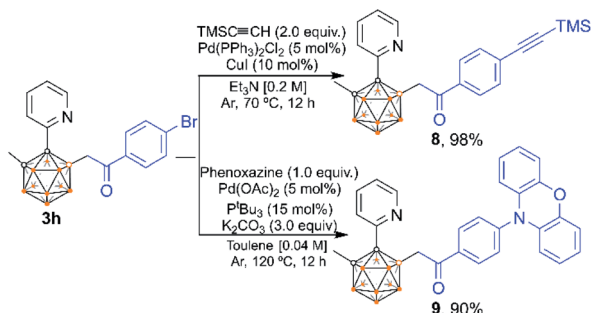
On the basis of the above results as well as literature reports,[9,15] a plausible reaction mechanism is depicted by using the reaction of **1a** and **4g** as an example (Scheme 9a). Firstly, the rhodium species RhCp*Cl$_2$ coordinates with the pyridyl group of **1a** to form intermediate **A** which subsequently induces B–H cleavage to generate a rhodacyclic complex **B** containing a Rh–B bond. Then **B** undergoes migratory insertion of α-carbonyl sulfoxonium ylide **4g** *via* a metal carbene intermediate **C** with loss of DMSO to give rise to **D**. This intermediate further delivers the final product **5g** *via* protodemetallation with concomitant regeneration of the RhCp*Cl$_2$ catalyst. It is noteworthy that the conversion between **D** and the product should be reversible as indicated by the deuteration experiment. This post-coordination between the mono-alkylated product and the rhodium catalyst can prohibit the iterative B–H activation pathway, and thus control the selective mono-substitution
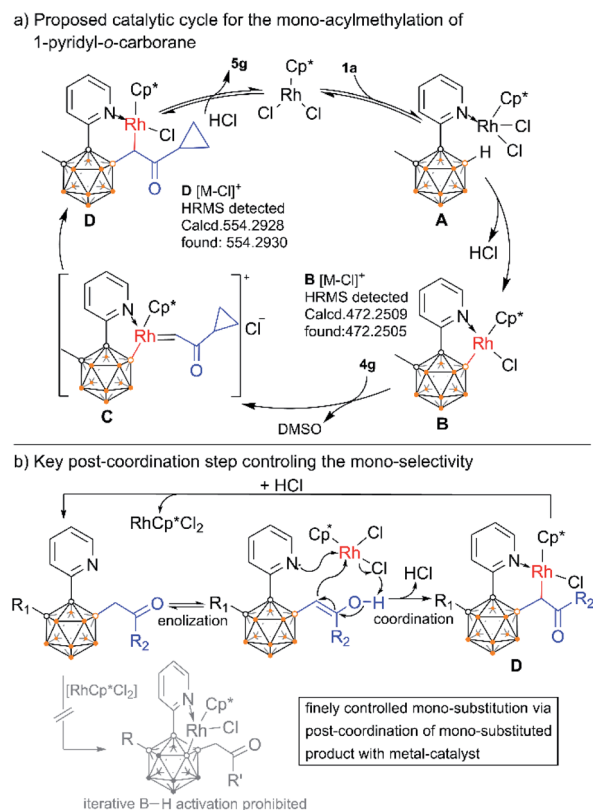
Scheme 9 Proposed reaction cycle for Rh(III)Cp*-catalyzed B(4)–H alkylation of *o*-carboranyl pyridine (a) and illustration of the post-coordination step (b).

(Scheme 9b). *In situ* NMR monitoring of the reaction suggests a clean catalytic conversion with the intermediacy of two new species, which may be related to **B** and **D** (ESI Fig. S23†). Trials to isolate these intermediates were unsuccessful. To our delight, HRMS measurements successfully detected the intermediates **B** and **D** across the different stages of the reaction (ESI Fig. S7–S22†). Furthermore, the α-deuterated analogue of **D** can also be detected in the deuteration reaction (ESI Fig. S27†). In addition, free DMSO liberated from sulfoxonium ylide was readily detected by ^{1}H NMR in the catalytic reaction mixture (ESI Fig. S31†). All these results support the proposed mechanism.

The utility of our method was developed. Compound **3h** can be further modified at its C–Br site (Scheme 10). Sonogashira coupling of **3h** with Me₃SiC≡CH afforded **8** in 98% isolated yield. The coupling reaction of **3h** with phenoxazine afforded product **9** in 90% isolated yield, which offers a new route to carborane B–H functionalized materials for potential application in light-emitting diodes. Note that C–H substituted carborane-based luminescent materials have been extensively studied,[3d–f,i,16] but there are few examples of studies involving B–H substituted carborane derivatives.[16b] Product **9** exhibits a significant aggregation-induced emission (AIE) effect as indicated by the photoluminescence (PL) spectra in THF/H₂O mixed solutions (Fig. 1, left). When the volumetric ratio of water (f_w vol%) reaches 80%, a light-yellow emission starts to appear at 525 nm, indicative of the AIE-behavior. A solvatochromic

phenomenon was observed as the emission peak exhibits a red shift from 457 nm (*n*-hexane) to 552 nm (CHCl₃) (Fig. 1, right).

The carbonyl functionality in the alkylated products provides an additional opportunity for post-functionalization at either the carbonyl site or its α-carbon position (Scheme 11). The carbonyl group in **5j** can be transformed into methylene by a borane reducing reagent, cleanly affording mono-alkylated product **10** (Scheme 11a). In addition, **3a** could be reduced to *o*-carboranyl aliphatic alcohol **11** in the presence of NaBH₄ which could be subsequently brominated and annulated with the 2-pyridyl group to provide carborane-fused quinolizinium. Deboronation at the B(6) position is observed in the isolated product, indicating the zwitterionic character of **12** (Scheme 11b). Besides the construction of quinoliziniums, carborane-fused indoliziniums can also be accessed by reacting the mono-acylmethylated products with Py·HBr₃ at 60 °C. This process involves one-pot bromination at the α-carbon (next to boron), and subsequent annulation with the 2-pyridyl group. A series of aryl substituted analogues are tolerated in this reaction, giving carborane-fused indoliziniums **13a–13e** in high yields (Scheme 11c). The alkyl group is not tolerated owing to

Scheme 10 Post-functionalization of **3h** via Pd-catalyzed cross-coupling reactions of C–Br bonds to form C–C and C–N bonds.
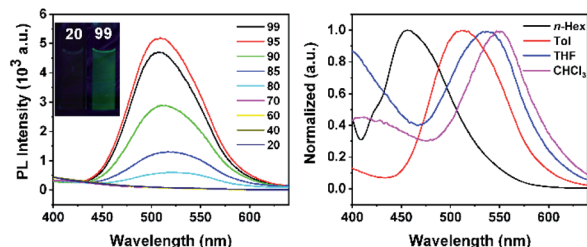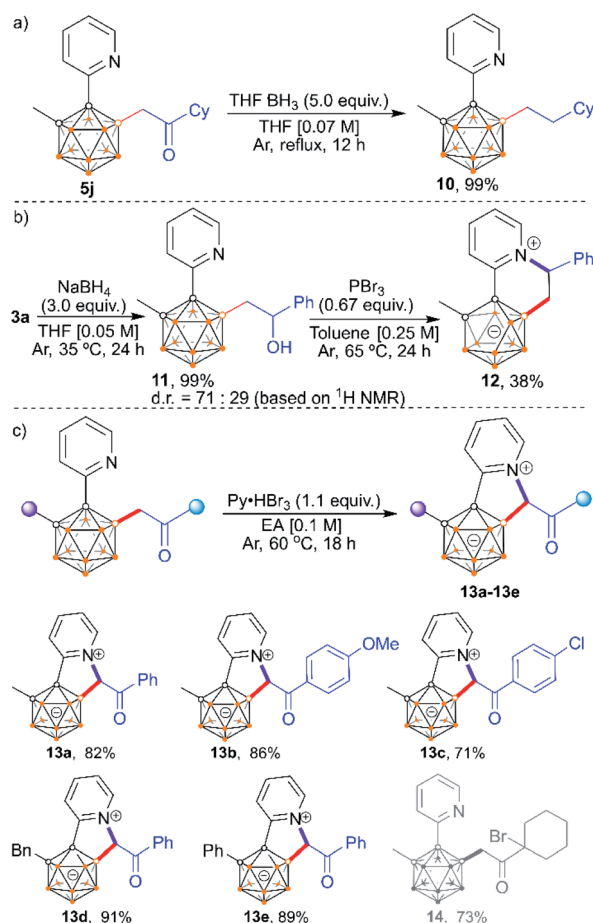

Fig. 1 Photophysical properties of **9**. (Left) Luminescence photographs taken under UV light (365 nm) and fluorescence spectra with different water volume fractions (v_H₂O/v_THF%) of **9** (1.0 × 10⁻⁵ M, λ_{ex} = 323 nm) under ambient conditions; (right) fluorescence spectra of **9** observed in different solvents (1.0 × 10⁻⁵ M, λ_{ex} = 323 nm) under ambient conditions.

Scheme 11 Post-functionalization. (a) Reduction of the carbonyl group to afford mono-alkylated carborane. (b) Synthesis of a carborane-fused quinolizinium. (c) Synthesis of carborane-fused indoliziniums.
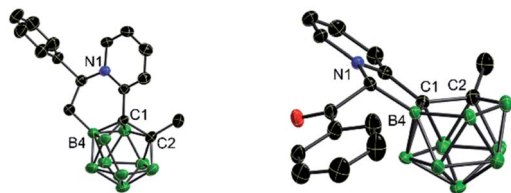
Fig. 2 X-ray structures of **12** (left) and **13a** (right).

competitive bromination at the other α-carbon position, as confirmed by the isolation of product **14** from the reaction with **5j**. It is also worth noting that the carbonyl functionality in the acylmethylated pyridylcarboranes is essential for the construction of carborane-fused indoliziniums as the carbonyl could activate the adjacent C–H unit.

Basically, the carborane-fused indoliziniums and quinoliziniums contain two diastereomers as indicated by their NMR spectra. The molecular structures of **12** and **13a** have been characterized by X-ray single crystal analysis (Fig. 2). The carboranyl group in the products is deboronated at the B(3)/B(6) position and the annulated compounds are zwitterionic. When comparing the crystal structures, it is obvious that the formation of compound **13a** proceeds through deboronation at the B(3) position, which is different from the formation of compound **12**. In the first case, it leads to B(9)-substituted nido-carborane, while in the second case it leads to B(4)-substituted nido-carborane. The ^{11}B NMR spectra also confirm this. Moreover, as far as we know, this is the first example of such deboronation. Interestingly, the carborane-fused quinoliziniums and indoliziniums display luminescence under UV irradiation. **12** and **13a** were selected as examples to investigate the photophysical properties (Fig. 3). Unexpectedly, the two compounds show efficient emission in the crystalline state and the emission wavelengths of the crystals are located in the yellowish green region (533 nm for **12** and 524 nm for **13a**, respectively). The absolute quantum yields of **12** and **13a** can reach 27% and 16%, respectively. In sharp contrast, those compounds prior to carborane fusion do not show emission either in solution or in the solid state, including the crystalline state. Obviously, the carborane-fused luminogens enable the aggregation caused quenching effect to be overcome. Recently,
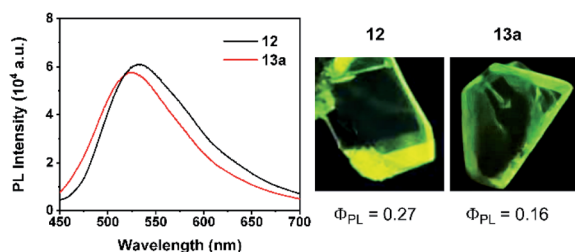
the synthesis of carborane-fused (hetero)arenes[3i,17] has provided a new opportunity for these boron-containing compounds as optoelectronic materials or drug candidates. The incorporation of the three-dimensional, aromatic and high boron-content carboranyl unit into these heteroarenes may offer promising value for drug design as well as other theranostic related biotechnologies.

Conclusions

In summary, we have presented an efficient metal-catalyzed selective B(4)/B(5)–H mono-acylmethylation protocol of pyridylcarboranes by using sulfoxonium ylides as the alkyl sources. The reaction shows broad substrate scope and gives access to a series of carborane-substituted carbonyl compounds with a B–C(sp^3) linkage at the α-carbon position. These products are difficult to synthesize by other means. The post-coordination of 2-pyridyl and enol moieties to the metal catalyst prohibits the iterative B–H activation event and leads to finely controlled mono-substitution. The products contain pyridyl, carbonyl and other newly incorporated organic functional groups, which provides new opportunities for post-functionalization. Notably, carborane-fused indoliziniums and quinoliziniums can be accessed, providing synthetic utility of this method in drug and luminescent molecule design.

Data availability

All experimental and crystallographic data are available in the ESI.†

Author contributions

H. Y. and H.-J. C. conceived and designed the present work. H.-J. C. and X. Z. wrote the manuscript. H. Y. and C. L. supervised the study. H.-J. C. performed and analyzed the experiments with assistance of X. W. and F. S. All authors contributed to the final manuscript.

Conflicts of interest

There are no conflicts to declare.

Acknowledgements

Fig. 3 Photophysical properties of **12** and **13a**. (Left) PL spectra (λ_{ex} = 365 nm) in the crystalline state under ambient conditions; (middle) luminescence photograph of the single crystal **12** taken under UV light (365 nm); (right) luminescence photograph of the single crystal **13a** taken under UV light (365 nm).

Notes and references

1 (*a*) R. N. Grimes, *Carboranes*, Academic Press, Amsterdam, 3rd edn, 2016; (*b*) N. S. Hosmane and R. Eagling, *Handbook of Boron Science*, World Scientific, Singapore, 2019.

2 For selected examples, see: (*a*) N. S. Hosmane and J. A. Maguire, in *Comprehensive Organometallic Chemistry*

III, ed. D. M. P. Mingos and R. H. Crabtree, Elsevier, Oxford, 2007, ch. 5, vol. 3; (*b*) P.-F. Cui, X.-R. Liu, S.-T. Guo, Y.-J. Lin and G.-X. Jin, *J. Am. Chem. Soc.*, 2021, **143**, 5099–5105; (*c*) I. B. Sivaev and V. I. Bregadze, *Coord. Chem. Rev.*, 2019, **392**, 146–176; (*d*) P. Coburger, S. Demeshko, C. Rödl, E. Hey-Hawkins and R. Wolf, *Angew. Chem., Int. Ed.*, 2017, **129**, 16087–16091; (*e*) B. J. Eleazer, M. D. Smith, A. A. Popov and D. V. Peryshkov, *J. Am. Chem. Soc.*, 2016, **138**, 10531–10538; (*f*) A. M. Spokoyny, C. W. Machan, D. J. Clingerman, M. S. Rosen, M. J. Wiester, R. D. Kennedy, C. L. Stern, A. A. Sarjeant and C. A. Mirkin, *Nat. Chem.*, 2011, **3**, 590–596; (*g*) X. Zhang, H. Dai, H. Yan, W. Zou and D. Cremer, *J. Am. Chem. Soc.*, 2016, **138**, 4334–4337; (*h*) H. Jude, H. Disteldorf, S. Fischer, T. Wedge, A. M. Hawkridge, A. M. Arif, M. F. Hawthorne, D. C. Muddiman and P. J. Stang, *J. Am. Chem. Soc.*, 2005, **127**, 12131–12139; (*i*) K. Jaiswal, N. Malik, B. Tumanskii, G. Ménard and R. Dobrovetsky, *J. Am. Chem. Soc.*, 2021, **143**, 9842–9848; (*j*) P. Coburger, J. Leitl, D. J. Scott, G. Hierlmeier, I. G. Shenderovich, E. Hey-Hawkins and R. Wolf, *Chem. Sci.*, 2021, 11225–11235; (*k*) H. D. A. C. Jayaweera, M. M. Rahman, P. J. Pellechia, M. D. Smith and D. V. Peryshkov, *Chem. Sci.*, 2021, 10441–10447; (*l*) R. Coult, M. A. Fox, W. R. Gill, P. L. Herbertson, J. A. H. MacBride and K. Wade, *J. Organomet. Chem.*, 1993, **462**, 19–29.

3 For selected examples, see: (*a*) L. Gan, A. Chidambaram, P. G. Fonquernie, M. E. Light, D. Choquesillo-Lazarte, H. Huang, E. Solano, J. Fraile, C. Viñas, F. Teixidor, J. A. R. Navarro, K. C. Stylianou and J. G. Planas, *J. Am. Chem. Soc.*, 2020, **142**, 8299–8311; (*b*) A. Saha, E. Oleshkevich, C. Vinas and F. Teixidor, *Adv. Mater.*, 2017, **29**, 1704238; (*c*) R. Nunez, I. Romero, F. Teixidor and C. Vinas, *Chem. Soc. Rev.*, 2016, **45**, 5147–5173; (*d*) X. Wei, M.-J. Zhu, Z. Cheng, M. Lee, H. Yan, C. Lu and J.-J. Xu, *Angew. Chem., Int. Ed.*, 2019, **58**, 3162–3166; (*e*) K.-R. Wee, Y.-J. Cho, J. K. Song and S. O. Kang, *Angew. Chem., Int. Ed.*, 2013, **52**, 9682–9685; (*f*) J. Ochi, K. Tanaka and Y. Chujo, *Angew. Chem., Int. Ed.*, 2020, **59**, 9841–9855; (*g*) B. P. Dash, R. Satapathy, E. R. Gaillard, J. A. Maguire and N. S. Hosmane, *J. Am. Chem. Soc.*, 2010, **132**, 6578–6587; (*h*) Y. Zhang, L. Yang, L. Wang, S. Duttwyler and H. Xing, *Angew. Chem., Int. Ed.*, 2019, **58**, 8145–8150; (*i*) R. Nunez, M. Tarres, A. Ferrer-Ugalde, F. F. de Biani and F. Teixidor, *Chem. Rev.*, 2016, **116**, 14307–14378; (*j*) D. Hablot, R. Ziessel, M. A. H. Alamiry, E. Bahraidah and A. Harriman, *Chem. Sci.*, 2013, **4**, 444–453; (*k*) K. O. Kirlikovali, J. C. Axtell, A. Gonzalez, A. C. Phung, S. I. Khan and A. M. Spokoyny, *Chem. Sci.*, 2016, **7**, 5132–5138; (*l*) X. Li, X. Tong, Y. Yin, H. Yan, C. Lu, W. Huang and Q. Zhao, *Chem. Sci.*, 2017, **8**, 5930–5940; (*m*) D. K. You, H. So, C. H. Ryu, M. Kim and K. M. Lee, *Chem. Sci.*, 2021, **12**, 8411–8423.

4 For selected examples, see: (*a*) T. Iijima, Y. Endo, M. Tsuji, E. Kawachi, H. Kagechika and K. Shudo, *Chem. Pharm. Bull.*, 1999, **47**, 398–404; (*b*) Z. J. Leśnikowski, *J. Med. Chem.*, 2016, **59**, 7738–7758; (*c*) N. P. E. Barry and

P. J. Sadler, *Chem. Soc. Rev.*, 2012, **41**, 3264–3279; (*d*) F. Issa, M. Kassiou and L. M. Rendina, *Chem. Rev.*, 2011, **111**, 5701–5722; (*e*) Y. Yin, N. Ochi, T. W. Craven, D. Baker, N. Takigawa and H. Suga, *J. Am. Chem. Soc.*, 2019, **141**, 19193–19197; (*f*) P. Stockmann, M. Gozzi, R. Kuhnert, M. B. Sárosi and E. Hey-Hawkins, *Chem. Soc. Rev.*, 2019, **48**, 3497–3512; (*g*) M. Scholz and E. Hey-Hawkins, *Chem. Rev.*, 2011, **111**, 7035–7062; (*h*) E. Hey-Hawkins and C. V. Teixidor, *Boron-Based Compounds: Potential and Emerging Applications in Medicine*, John Wiley & Sons, 2018; (*i*) R. Otero, S. Seoane, R. Sigüeiro, A. Y. Belorusova, M. A. Maestro, R. Pérez-Fernández, N. Rochel and A. Mouriño, *Chem. Sci.*, 2016, **7**, 1033–1037; (*j*) K. Fujiki, Y. Kanayama, S. Yano, N. Sato, T. Yokokita, P. Ahmadi, Y. Watanabe, H. Haba and K. Tanaka, *Chem. Sci.*, 2019, **10**, 1936–1944; (*k*) M. Couto, C. Alamón, S. Nievas, M. Perona, M. A. Dagrosa, F. Teixidor, P. Cabral, C. Viñas and H. Cerecetto, *Chem.–Eur. J.*, 2020, **26**, 14335–14340; (*l*) M. Couto, C. Alamón, M. F. García, M. Kovacs, E. Trias, S. Nievas, E. Pozzi, P. Curotto, S. Thorp, M. A. Dagrosa, F. Teixidor, C. Viñas and H. Cerecetto, *Cells*, 2020, **9**, 1408.

5 For related reviews, see: (*a*) Y. Quan and Z. Xie, *Chem. Soc. Rev.*, 2019, **48**, 3660–3673; (*b*) S. Duttwyler, *Pure Appl. Chem.*, 2018, **90**, 733–744; (*c*) X. Zhang and H. Yan, *Coord. Chem. Rev.*, 2019, **378**, 466–482; (*d*) W.-B. Yu, P.-F. Cui, W.-X. Gao and G.-X. Jin, *Coord. Chem. Rev.*, 2017, **350**, 300–319; (*e*) Y. K. Au and Z. Xie, *Bull. Chem. Soc. Jpn.*, 2021, **94**, 879–899.

6 For selected examples, see: (*a*) W. Jiang, C. B. Knobler, M. D. Mortimer and M. F. Hawthorne, *Angew. Chem., Int. Ed.*, 1995, **34**, 1332–1334; (*b*) B. T. King, Z. Janoušek, B. Grüner, M. Trammell, B. C. Noll and J. Michl, *J. Am. Chem. Soc.*, 1996, **118**, 3313–3314; (*c*) J. D. Hewes, C. W. Kreimendahl, T. B. Marder and M. F. Hawthorne, *J. Am. Chem. Soc.*, 1984, **106**, 5757–5759; (*d*) Q. Wang, S. Tian, C. Zhang, J. Li, Z. Wang, Y. Du, L. Zhou and J. Lu, *Org. Lett.*, 2019, **21**, 8018–8021; (*e*) C. Tang, J. Zhang and Z. Xie, *Angew. Chem., Int. Ed.*, 2017, **56**, 8642–8646; (*f*) C. Tang, J. Zhang, J. Zhang and Z. Xie, *J. Am. Chem. Soc.*, 2018, **140**, 16423–16427; (*g*) X. Zhang, H. Zheng, J. Li, F. Xu, J. Zhao and H. Yan, *J. Am. Chem. Soc.*, 2017, **139**, 14511–14517; (*h*) X. Zhang and H. Yan, *Chem. Sci.*, 2018, **9**, 3964–3969; (*i*) Z.-Y. Zhang, X. Zhang, J. Yuan, C.-D. Yue, S. Meng, J. Chen, G.-A. Yu and C.-M. Che, *Chem.–Eur. J.*, 2020, **26**, 5037–5050; (*j*) Y.-F. Liang, L. Yang, B. B. Jei, R. Kuniyil and L. Ackermann, *Chem. Sci.*, 2020, 10764–10769; (*k*) T.-T. Xu, K. Cao, C.-Y. Zhang, J. Wu, L.-F. Ding and J. Yang, *Org. Lett.*, 2019, **21**, 9276–9279; (*l*) F. Lin, J.-L. Yu, Y. Shen, S.-Q. Zhang, B. Spingler, J. Liu, X. Hong and S. Duttwyler, *J. Am. Chem. Soc.*, 2018, **140**, 13798–13807; (*m*) M. G. L. Mirabelli and L. G. Sneddon, *J. Am. Chem. Soc.*, 1988, **110**, 449–453; (*n*) Y. Shen, K. Zhang, X. Liang, R. Dontha and S. Duttwyler, *Chem. Sci.*, 2019, **10**, 4177–4184; (*o*) Y. Zhang, Y. Sun, F. Lin, J. Liu and S. Duttwyler, *Angew. Chem., Int. Ed.*, 2016, **55**, 15609–15614; (*p*) F. Teixidor, G. Barberà, A. Vaca, R. Kivekäs, R. Sillanpää, J. Oliva and C. Viñas, *J. Am. Chem. Soc.*, 2005, **127**, 10158–

10159; (*q*) A. V. Puga, F. Teixidor, R. Sillanpää, R. Kivekäs and C. Viñas, *Chem. Commun.*, 2011, **47**, 2252–2254.

7 C. Guo, Z. Qiu and Z. Xie, *ACS Catal.*, 2021, **11**, 2134–2140.

8 For selected examples, see: (*a*) M. W. Lee, Jr., Y. V. Sevryugina, A. Khan and S. Q. Ye, *J. Med. Chem.*, 2012, **55**, 7290–7294; (*b*) M. Koshino, T. Tanaka, N. Solin, K. Suenaga, H. Isobe and E. Nakamura, *Science*, 2007, **316**, 853; (*c*) L. Kobr, K. Zhao, Y. Shen, A. Comotti, S. Bracco, R. K. Shoemaker, P. Sozzani, N. A. Clark, J. C. Price, C. T. Rogers and J. Michl, *J. Am. Chem. Soc.*, 2012, **134**, 10122–10131; (*d*) J. Wang, L. Chen, J. Ye, Z. Li, H. Jiang, H. Yan, M. Y. Stogniy, I. B. Sivaev, V. I. Bregadze and X. Wang, *Biomacromolecules*, 2017, **18**, 1466–1472.

9 For selected examples, see: (*a*) T. Zhou, P.-F. Qian, J.-Y. Li, Y.-B. Zhou, H.-C. Li, H.-Y. Chen and B.-F. Shi, *J. Am. Chem. Soc.*, 2021, **143**, 6810–6816; (*b*) P. B. Momo, A. N. Leveille, E. H. E. Farrar, M. N. Grayson, A. E. Mattson and A. C. B. Burtoloso, *Angew. Chem., Int. Ed.*, 2020, **59**, 15554–15559; (*c*) M. Barday, C. Janot, N. R. Halcovitch, J. Muir and C. Aissa, *Angew. Chem., Int. Ed.*, 2017, **56**, 13117–13121; (*d*) J. Vaitla, A. Bayer and K. H. Hopmann, *Angew. Chem., Int. Ed.*, 2017, **56**, 4277–4281; (*e*) Y. W. Xu, X. K. Zhou, G. F. Zheng and X. W. Li, *Org. Lett.*, 2017, **19**, 5256–5259.

10 For selected examples, see: (*a*) J. J. Li, *Heterocyclic Chemistry in Drug Discovery*, John Wiley & Sons, Hoboken, 2013; (*b*) S. Banerjee, E. B. Veale, C. M. Phelan, S. A. Murphy, G. M. Tocci, L. J. Gillespie, D. O. Frimannsson, J. M. Kelly and T. Gunnlaugsson, *Chem. Soc. Rev.*, 2013, **42**, 1601–1618; (*c*) S. Basili, A. Bergen, F. Dall'Acqua, A. Faccio, A. Granzhan, H. Ihmels, S. Moro and G. Viola, *Biochemistry*, 2007, **46**, 12721–12736; (*d*) A. Rescifina, C. Zagni, M. G. Varrica, V. Pistarà and A. Corsaro, *Eur. J. Med. Chem.*, 2014, **74**, 95–115.

11 For selected examples, see: (*a*) K. Iwasa, H.-S. Kim, Y. Wataya and D.-U. Lee, *Eur. J. Med. Chem.*, 1998, **33**, 65–69; (*b*) K. Iwasa, Y. Nishiyama, M. Ichimaru, M. Moriyasu, H.-S. Kim, Y. Wataya, T. Yamori, T. Takashi and D.-U. Lee, *Eur. J. Med. Chem.*, 1999, **34**, 1077–1083.

12 For selected examples, see: (*a*) E. Jortzik, K. Zocher, A. Isernhagen, B. M. Mailu, S. Rahlfs, G. Viola, S. Wittlin, N. H. Hunt, H. Ihmels and K. Becker, *Antimicrob. Agents Chemother.*, 2016, **60**, 115–125; (*b*) D. Morisaki, H.-S. Kim, H. Inoue, H. Terauchi, S. Kuge, A. Naganuma, Y. Wataya, H. Tokuyama, M. Ihara and K. Takasu, *Chem. Sci.*, 2010, **1**, 206–209; (*c*) K. Takasu, D. Morisaki, M. Kaiser, R. Brun and M. Ihara, *Heterocycles*, 2005, **66**, 161–166.

13 S. S. Kolli, D. Pecone, A. Pona, A. Cline and S. R. Feldman, *Am. J. Clin. Dermatol.*, 2019, **20**, 345–365.

14 (*a*) Z. He, A. Zajdlik and A. K. Yudin, *Dalton Trans.*, 2014, **43**, 11434–11451; (*b*) D. B. Diaz, C. C. G. Scully, S. K. Liew, S. Adachi, P. Trinchera, J. D. St Denis and A. K. Yudin, *Angew. Chem., Int. Ed.*, 2016, **55**, 12659–12663; (*c*) P. Trinchera, V. B. Corless and A. K. Yudin, *Angew. Chem., Int. Ed.*, 2015, **54**, 9038–9041; (*d*) Z. He and A. K. Yudin, *J. Am. Chem. Soc.*, 2011, **133**, 13770–13773; (*e*) J. D. St. Denis, Z. He and A. K. Yudin, *ACS Catal.*, 2015, **5**, 5373–5379.

15 (*a*) Q. Zhang and B.-F. Shi, *Acc. Chem. Res.*, 2021, **54**, 2750–2763; (*b*) P. Hu, L. Kong, F. Wang, X. Zhu and X. Li, *Angew. Chem., Int. Ed.*, 2021, **60**, 20424–20429; (*c*) L. Sun, H. Chen, B. Liu, J. Chang, L. Kong, F. Wang, Y. Lan and X. Li, *Angew. Chem., Int. Ed.*, 2021, **60**, 8391–8395.

16 (*a*) X. Li, X. Tong, H. Yan, C. Lu, Q. Zhao and W. Huang, *Chem.–Eur. J.*, 2016, **22**, 17282–17290; (*b*) B. P. Dash, R. Satapathy, E. R. Gaillard, J. A. Maguire and N. S. Hosmane, *J. Am. Chem. Soc.*, 2010, **132**, 6578–6587.

17 For selected examples, see: (*a*) Z. Yang, W. Zhao, W. Liu, X. Wei, M. Chen, X. Zhang, X. Zhang, Y. Liang, C. Lu and H. Yan, *Angew. Chem., Int. Ed.*, 2019, **58**, 11886–11892; (*b*) Y. Sun, J. Zhang, Y. Zhang, J. Liu, S. van der Veen and S. Duttwyler, *Chem.–Eur. J.*, 2018, **24**, 10364–10371.